Improved Air Quality Forecasting
Invest to Save Report ISB52-02

Boundary layer meteorology by pulsed lidar

By

GN Pearson, DV Willetts & RI Young

QinetiQ

16 April 2002

Authorisation

Prepared by	Dr RI Young
Title	
Signature	
Date	April 2002
Location	QinetiQ Malvern

Principal authors	Prof DV Willetts
Appointment	Technical Leader, Remote Sensing
	QinetiQ
Principal authors	Dr GN Pearson
Appointment	QinetiQ Fellow, Remote Sensing
Location	QinetiQ
Principal authors	Dr RI Young
Appointment	Project Manger, Remote Sensing
Location	QinetiQ

Record of changes

Issue	Date	Detail of Changes
1.0	16 April 2002	First Release

ABSTRACT

This report ISB52-02 was produced under Project 52 of the Invest to Save Scheme, or ISB.

The objective of this project is to improve the Met Office air quality forecast service and thus impact on the quality of life in and around urban areas. To achieve this the Project seeks to gather and exploit observations from two unique Doppler lidar systems within the framework provided by an operational air quality numerical forecasting model. The data set will provide information on the four dimensional nature of turbulence in the atmospheric boundary layer in the vicinity of an urban area. Through comparisons of these data with numerical models of the turbulence, improvements in the structure of an operational air quality forecasting model will be specified.

Prior to making the measurements both lidars needed their range performance upgraded. This report gives details of a preliminary set of measurements made at QinetiQ Malvern using the recently upgraded Salford University pulsed lidar.

List of contents

1. INTRODUCTION

Pulsed Doppler lidar can monitor the wind by detecting backscattered light from naturally occurring aerosol particles which act as tracers embedded in the atmosphere. The system measures the Doppler shift between the outgoing and return radiation and consequently determines the line-of-sight component of the wind velocity. Range resolution is ultimately determined by the pulse length but factors such as the length of the time series taken for each rangegate and the processing algorithms employed also effect the range resolution. The heterodyne receiver configuration, when operated in the shot noise limit, gives essentially quantum limited performance in the IR where background light and detector noise would otherwise limit the sensitivity.

2. EQUIPMENT DESCRIPTION

A major part of the work being undertaken in this project is the upgrade to the existing Q-switched lidar system. The upgrade involves new transmitter technology, allowing the output power to be increased by two orders of magnitude. A somewhat similar upgrade has now been completed (using quite separate funding) on the sister equipment which will be used to provide the second lidar system for the trials in this project. Figure (1) shows a schematic drawing of the optical layout and figures (2-3) show photographs of the lidar. The transmitter and local oscillator lasers are housed within a common invar frame structure to ensure a high degree of passive stability. The transmitter is a hybrid design where a high energy pulsed gain module is combined with a cw discharge section in the same resonator. We have employed a "U-fold" configuration for compactness. The local oscillator (LO) and transmitter resonators both use a Littrow mounted diffraction grating for line selection and were set to operate on the P(2O) transition at a wavelength of 10.591μm. A dedicated computer monitors the outputs of both these lasers (via detectors D1 and D2) and controls their operation. The same computer also controls the pulse repetition rate and the triggering. This is done with custom hardware and software. The software user interface is shown in figure (4) and the custom hardware board is shown in figure (5).

The basic principle for the computer control of the lasers is as follows. A dither is applied to the Piezoelectric tube (PZT) upon which the transmitter laser output coupling mirror is mounted. This dither is 170mV in amplitude and is at a frequency of 673Hz. This results in a displacement dither on the laser mirror of approximately $\pm$ 9nm. The optical frequency dither induced by this motion is approximately $\pm$ 250kHz. Since the gain bandwidth in continuous wave mode is only ~100MHz, this frequency dither gives rise to a small amplitude dither on the laser output and this is detected by D1. The signal is then filtered and fed to a phase sensitive amplifier (PSA) referenced to the original dither voltage. The phase of the PSA output is then used in a feedback loop to hold the laser at peak power which is approximately line centre. D1 also receives radiation from the CW LO and this beats with the transmitter output. This beat frequency is amplified and then passed through an electronic discriminator which has an output centred at 12MHz and a response of –0.5 V MHz^{-1}. The output of this device is then used as the error signal in a second servo loop which holds the LO laser 12MHz away from the transmitter, thus defining the receiver IF as 12MHz.

The backscattered radiation is detected by D3. This signal is amplified and sent to the data acquisition (DA) computer. A reference signal for each laser shot is detected by D2 and this signal is also sent to the DA computer.

The signal is now processed in real-time by this computer in contrast to the previous system where the raw data was stored for off-line processing. The range gate length, maximum range, number of shots to average and number of accumulation sets are entered into the programme. Once a noise file has been taken the acquisition button is pressed and data set is taken. The size of the files is reduced with respect to the raw data storage mode used previously. Half an hour's worth of data out to 9km range with 8 seconds of averaging per set occupies ~ 350 kbytes.

3. CONVECTIVE BOUNDARY LAYER DATA, 27/03/02

We show here some initial data obtained using this equipment to allow the reader to appreciate potential performance in the ISB52 project. The system was **unscanned**, set to observe continuously in the 080 degrees direction which was arranged to be very close to downwind at the beginning of the measurement. As a consequence the observations were collected from above a flat region of the Severn Plain to the east of the Malvern Hills. The sightline was set to an elevation of 7.5 degrees above horizontal, and velocity was calculated in 112m rangegates. Instrumental narcissus limited the minimum range to about 1.1km (150m AGL), while beyond about 7 km range (900m AGL) the signal to noise ratio was usually too low to allow good estimates of velocity to be computed. This maximum range is a function of atmospheric scattering and transmission, but is clearly three to four times that achievable before upgrade. The system was operated at a 10Hz pulse repetition frequency and 80 pulses were integrated in each individual experiment, which therefore lasted 8 seconds. The measured sightline velocity v_m in each rangegate for this configuration is given by

$$v_m = v_h \cos 7.5 + w \sin 7.5 = 0.99v_h + 0.13w$$

where v_h is the horizontal component of velocity in the vertical plane containing the sightline, and w is the vertical component. Thus the sightline velocity consists of 88% horizontal motion and 12% vertical.

The composite pressure & cloud chart is shown in figure (6), and figure (7) shows visible and IR satellite images. Figure (8) shows a photograph taken in the approximate direction of the lidar beam at 1730.

Figures (9-18) show colour coded velocity data acquired on 27 March 2002, plotted as a function of range (height) against time, beginning before dawn and concluding after sunset. Many features of meteorological interest are evident and we append tentative assignments below. On the accompanying diagram, in which all four digit numbers are GMT times, positive velocities are towards the instrument, negative velocities are away from the instrument.

At the outset, at 0425, there is a background flow of about -2.5m/s, embedded in which there is a windshear or nocturnal jet at about 600m AGL, having a velocity of around -3.5m/s. By 0500 a second jet has developed at about 300m AGL, with a similar speed. Both tend to die out near dawn at about 0630, but the lower one continues feebly and bifurcates at about 0715 into 300 and 400m levels. The higher one fades out at about 0830 while the lower gradually descends to about 250m by 0930 and then fades away.

At altitudes of 700 - 800m AGL a flow reversal to about +2m/s begins to appear from around dawn at about 0600, and this region thickens progressively to at least 100m at 0900. By about 1000 instabilities are developing in the shear layer and a possible boundary layer folding event takes place near 1100. At this time strong convective activity commences, with features such as that between 1140 and 1230 being consistent with advection of turbulent billows by the background windfield. This activity peaks with sightline velocity fluctuations of about 6m/s, but gradually weakens during the afternoon, and the background wind falls to about -1m/s. By sunset at about 1810, the convection has ceased and at levels below about 400m AGL flow begins towards the instrument, of about +1m/s, while at greater altitudes flows of -2m/s are evident. This situation prevailed until the experiment ceased at 1905.

Figure (19) shows the effect of scanning the beam in elevation. At the end of the day the beam was scanned with a view to checking the height distribution of the backscatter. The range/Doppler/time (angle) plot is shown together with the range/intensity/time (angle) plot. It can be seen that as the beam angle is reduced, the maximum range for good Doppler estimates increases. The intensity shows a similar increase. This indicates that the

backscatter distribution with height has a relatively sharp edge at the height of the maximum range which perhaps indicates the boundary layer height.

Similar systems have been operated elsewhere, notably at NOAA Boulder, but to the authors' knowledge such structures have not been observed previously in the clear air. It is believed that there are a number of reasons for this; for instance this equipment produces better velocity estimates, and previous work has involved scanning, which will smear convective cell information. Clearly there is the potential to acquire new insights into mesoscale meteorological phenomena, and the use of two such systems in ISB52 to give 3D windfields will allow major advances in understanding boundary layer dynamics, turbulence, and pollution transport.

4. SUMMARY

1. The Project represents a unique opportunity to gain flow and turbulence data using lidar remote sensing over a city for the improvement of dispersion models that are used in air quality forecasting. Current experience in the Met Office shows that the required measurement heights and spatial sampling over a conurbation can only be achieved through the use of pulsed lidar remote sensing techniques. However current lidar technology needs to be upgraded to meet the required range demands.
2. This report describes recent lidar implementations made at Malvern upon the Salford Pulsed lidar. They are typical of the upgrades shortly to be made to the Malvern pulsed lidar.
3. Further to this the performance of the upgraded lidar and a set of measurements that have been made by the lidar along a fixed line of sight over the Severn Plain are presented.
4. The results demonstrate the ability of a pulsed lidar to observe mesoscale meteorological phenomena.
5. Further work is now required to evaluate these lidar observations in comparison with meteorological data gathered from other sources or predictions made by simulations. A key objective is then to understand the lidar data in terms of the physical processes of the mesoscale meteorological phenomena.
6. From this the key flow visualisation parameters can be identified allowing the specification of the field scanning/sampling programme.
7. The results from this further work will be presented in the following milestone, MS3, due in October 2002.

This report is the second Milestone in the ISB Urban Lidar Project No 52.

5 FIGURES

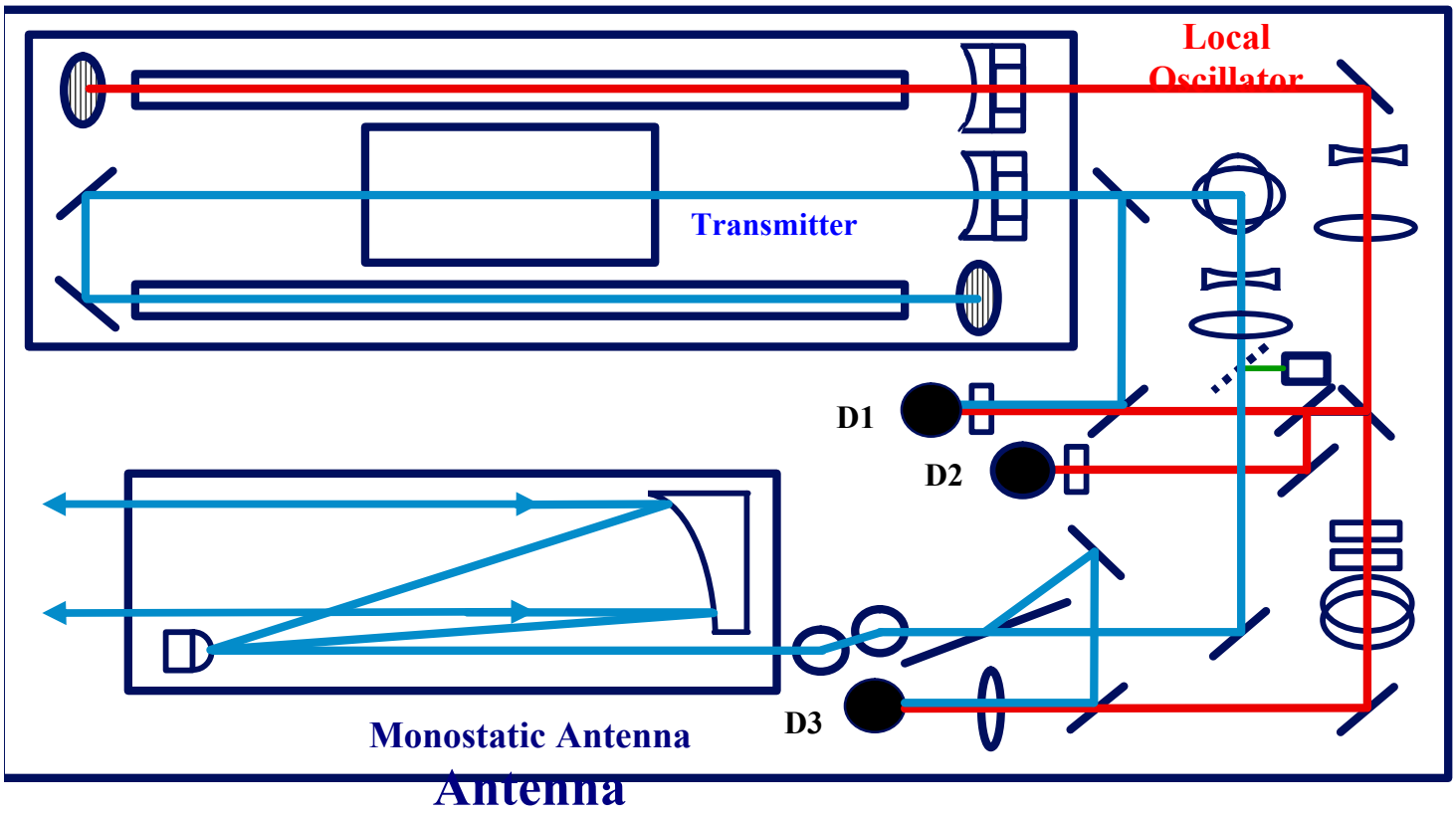

Figure (1) A schematic diagram of the optical layout of the lidar

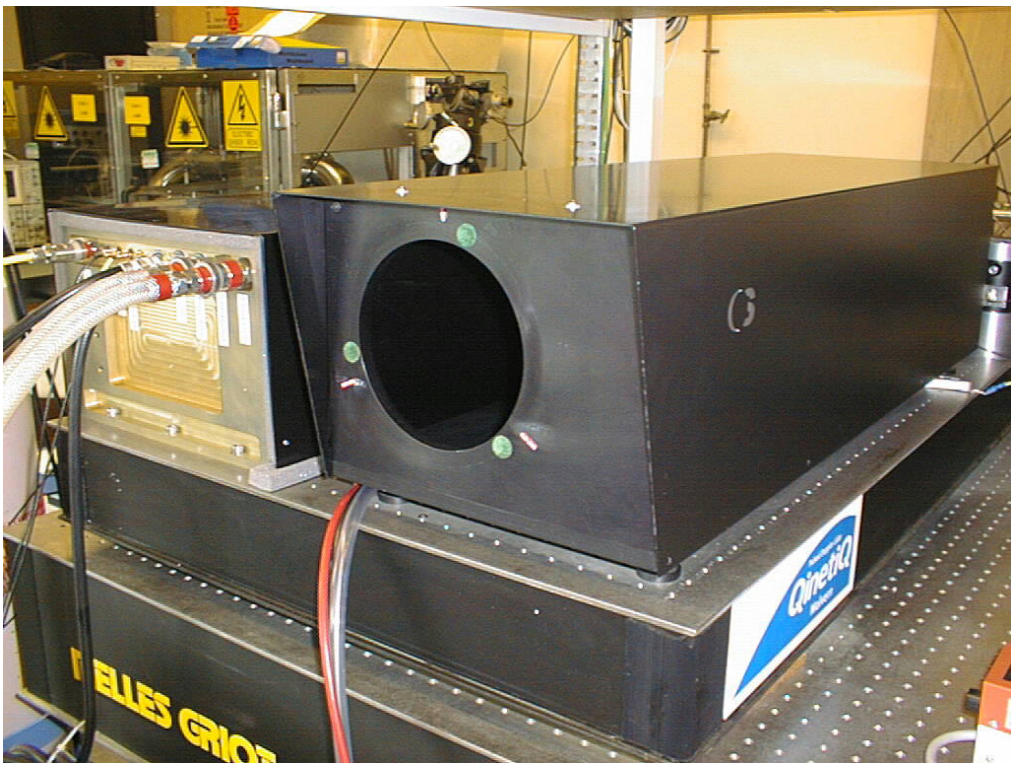

Figure (2) A photograph of the lidar showing the output aperture and the laser power/coolant connections

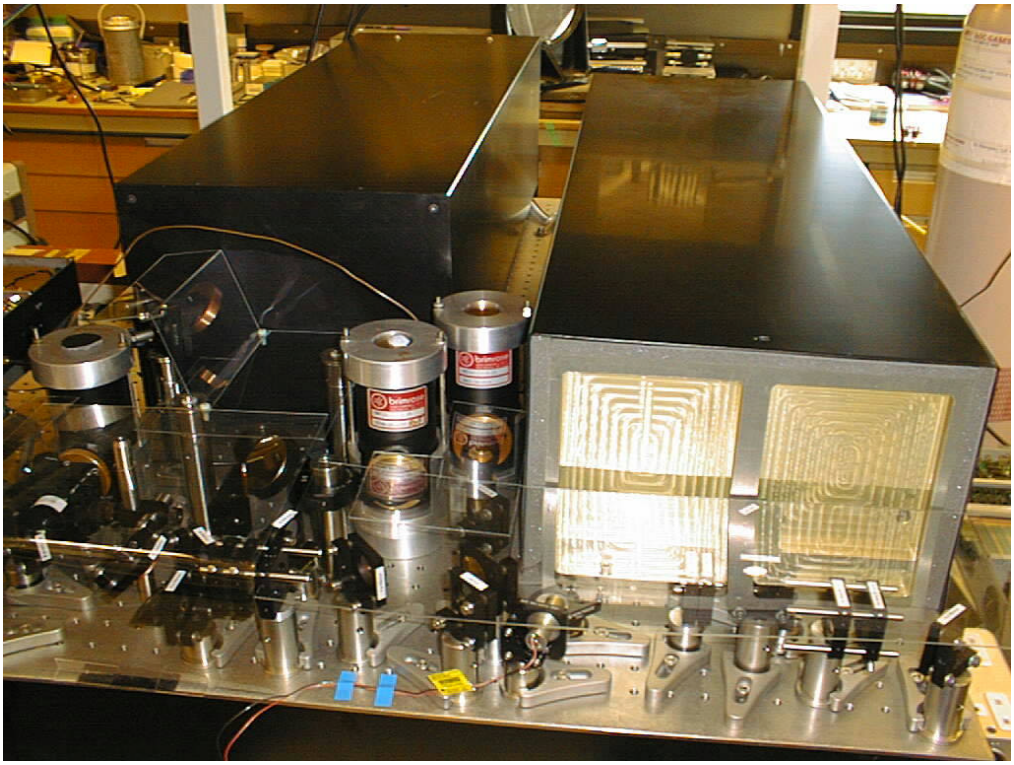

Figure (3) A photograph of the lidar showing the laser enclosure, the optical mounts, the detectors and the telescope.

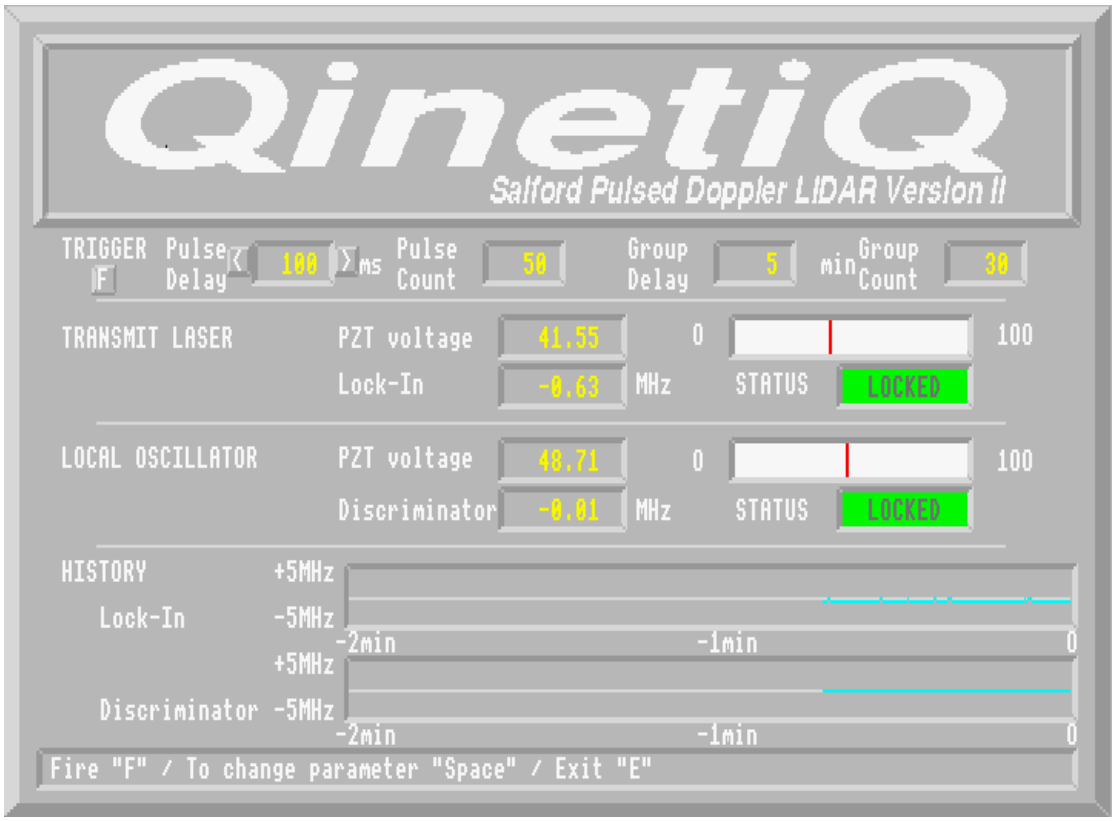

Figure (4) The user interface of the control software

Figure (5) A photograph of the custom-made control board

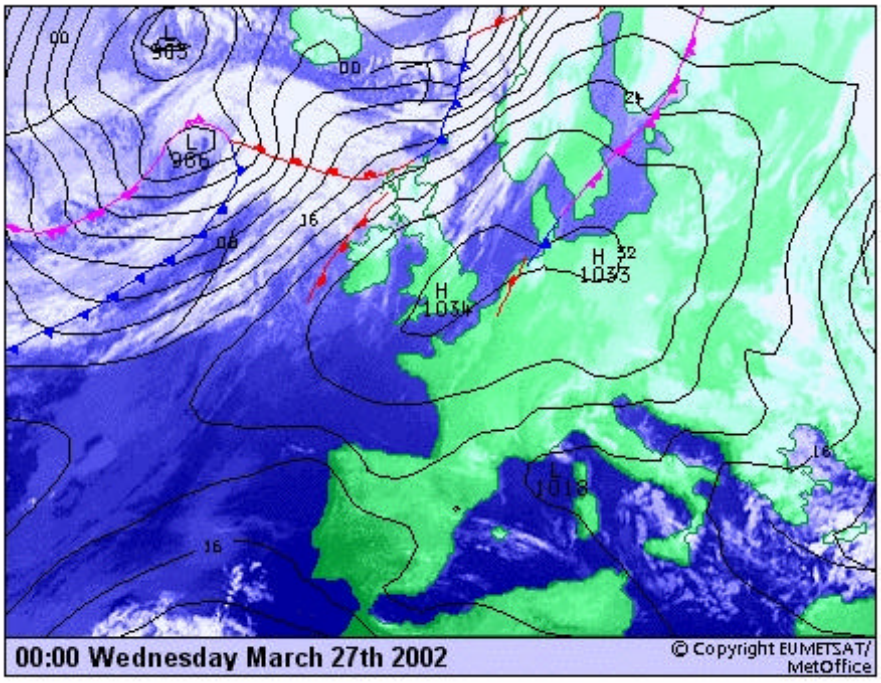

Figure (6) The pressure & cloud composite for 27/03/02

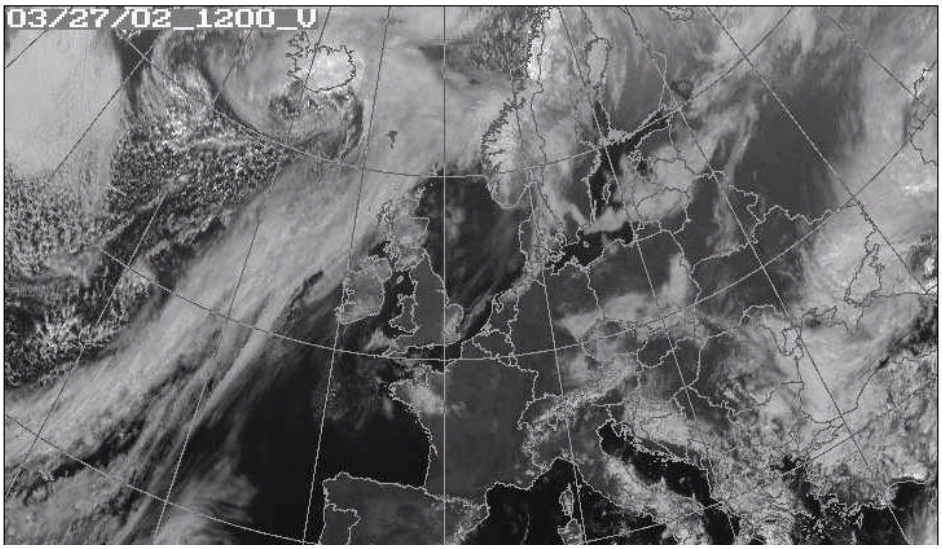

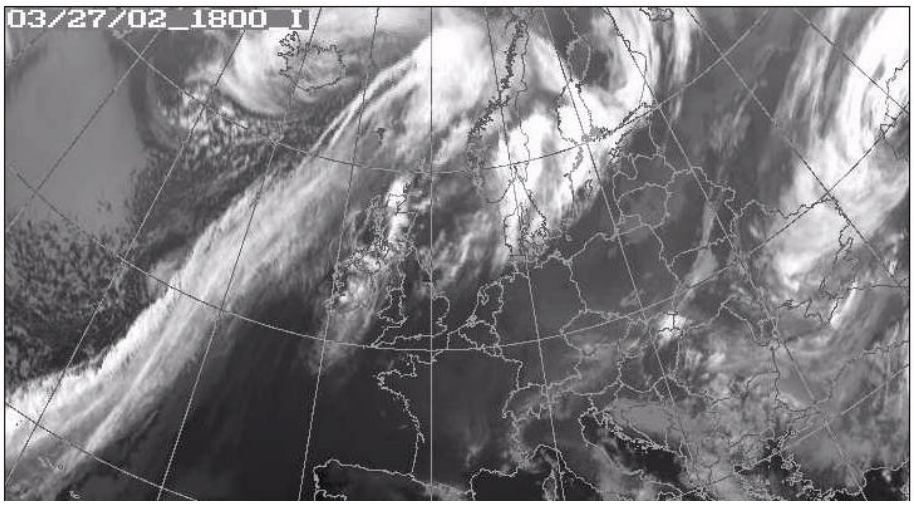

Figure (7) Visible and IR satellite images

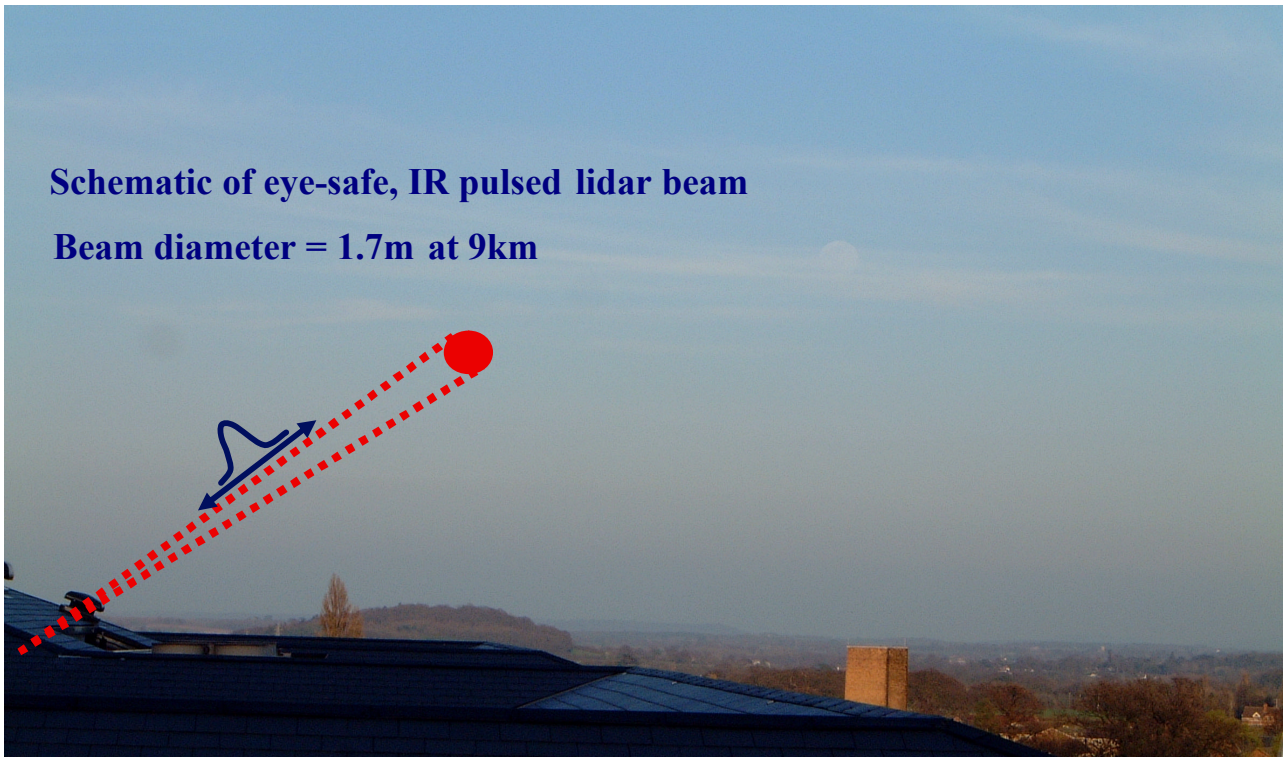

Figure (8) A photograph taken out over the Severn plain at 1730

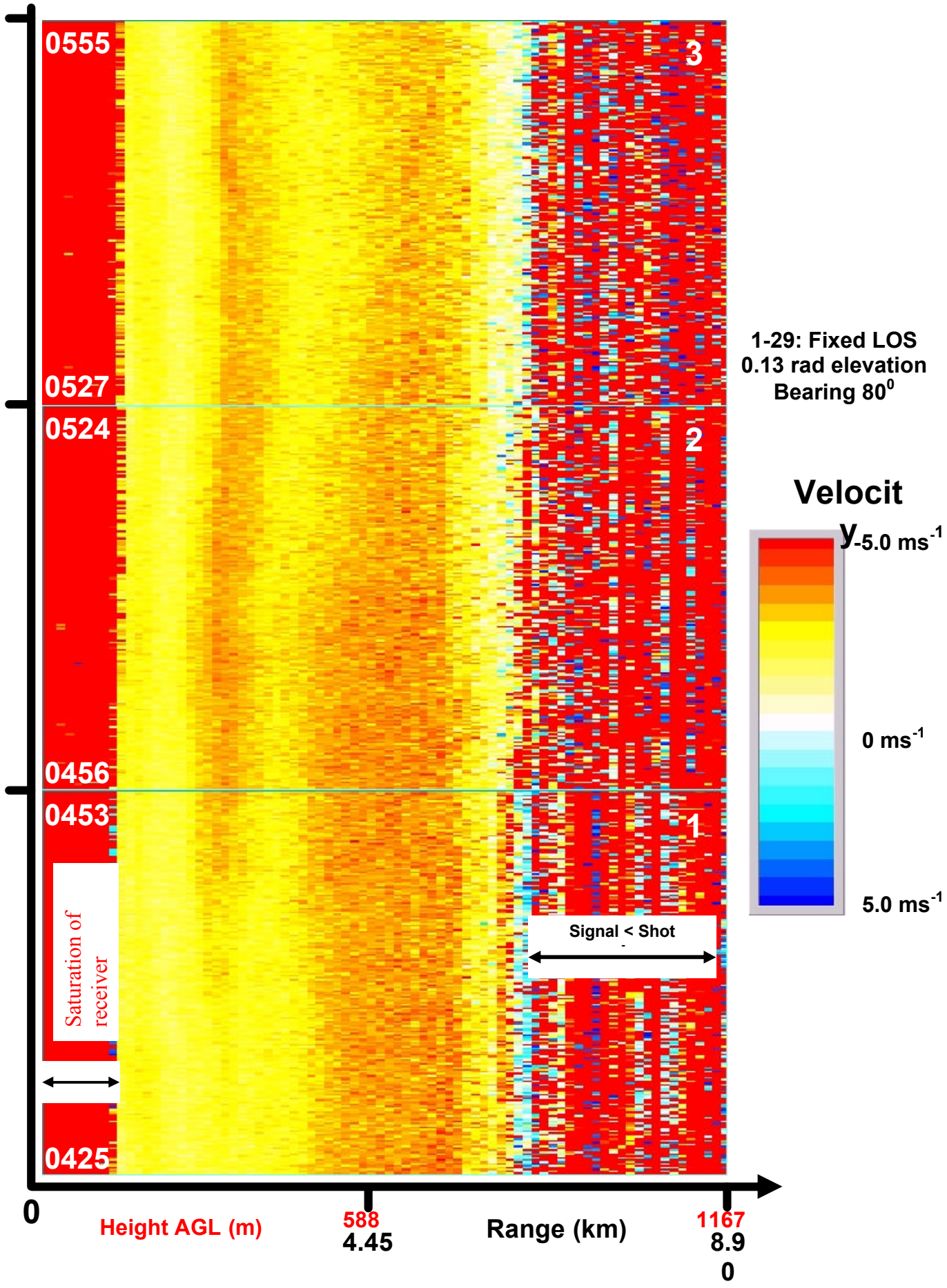

Figure (9) Range vs Velocity vs Time (start and stop times in white)

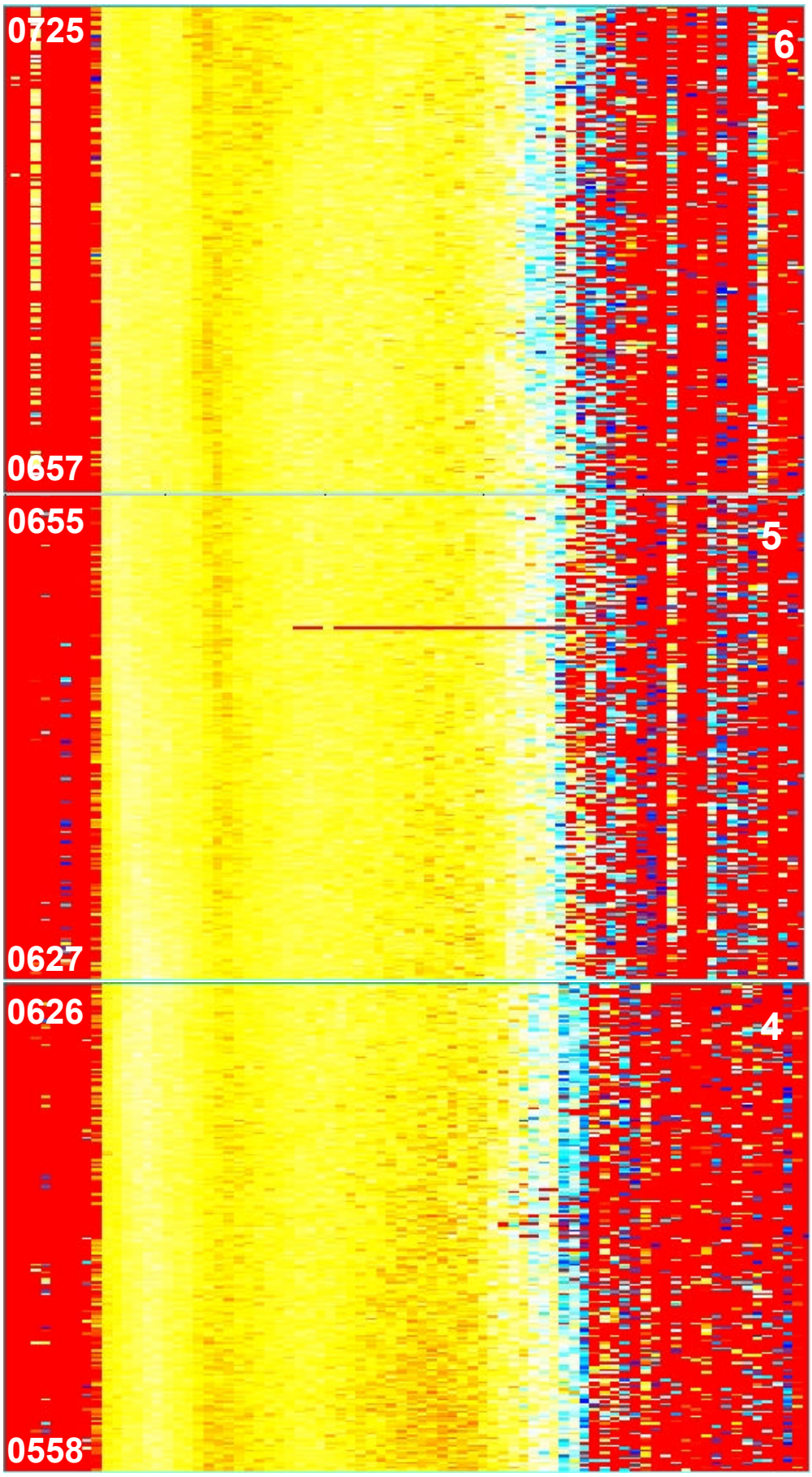

Figure (10) Range vs Velocity vs Time

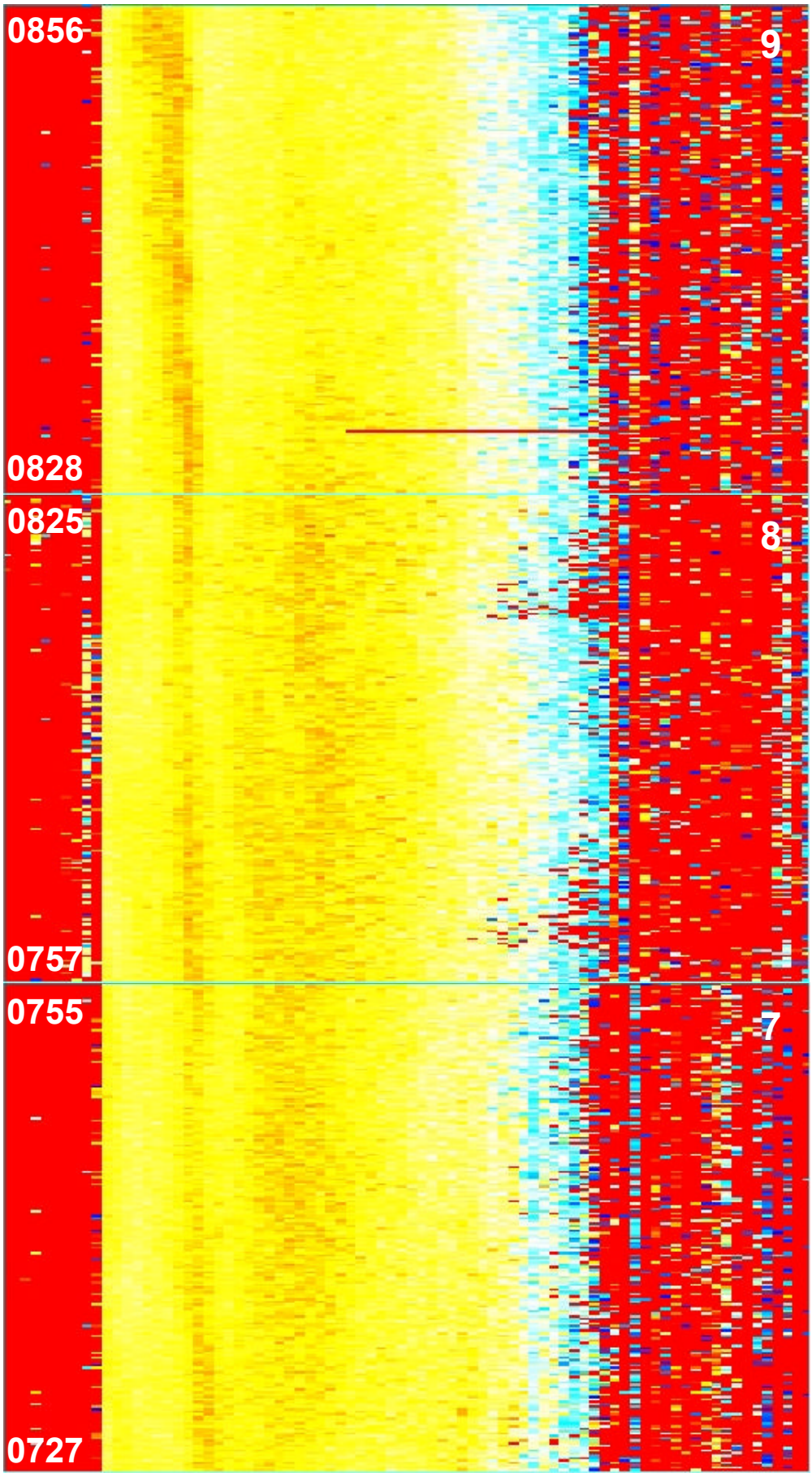

Figure (11) Range vs Velocity vs Time

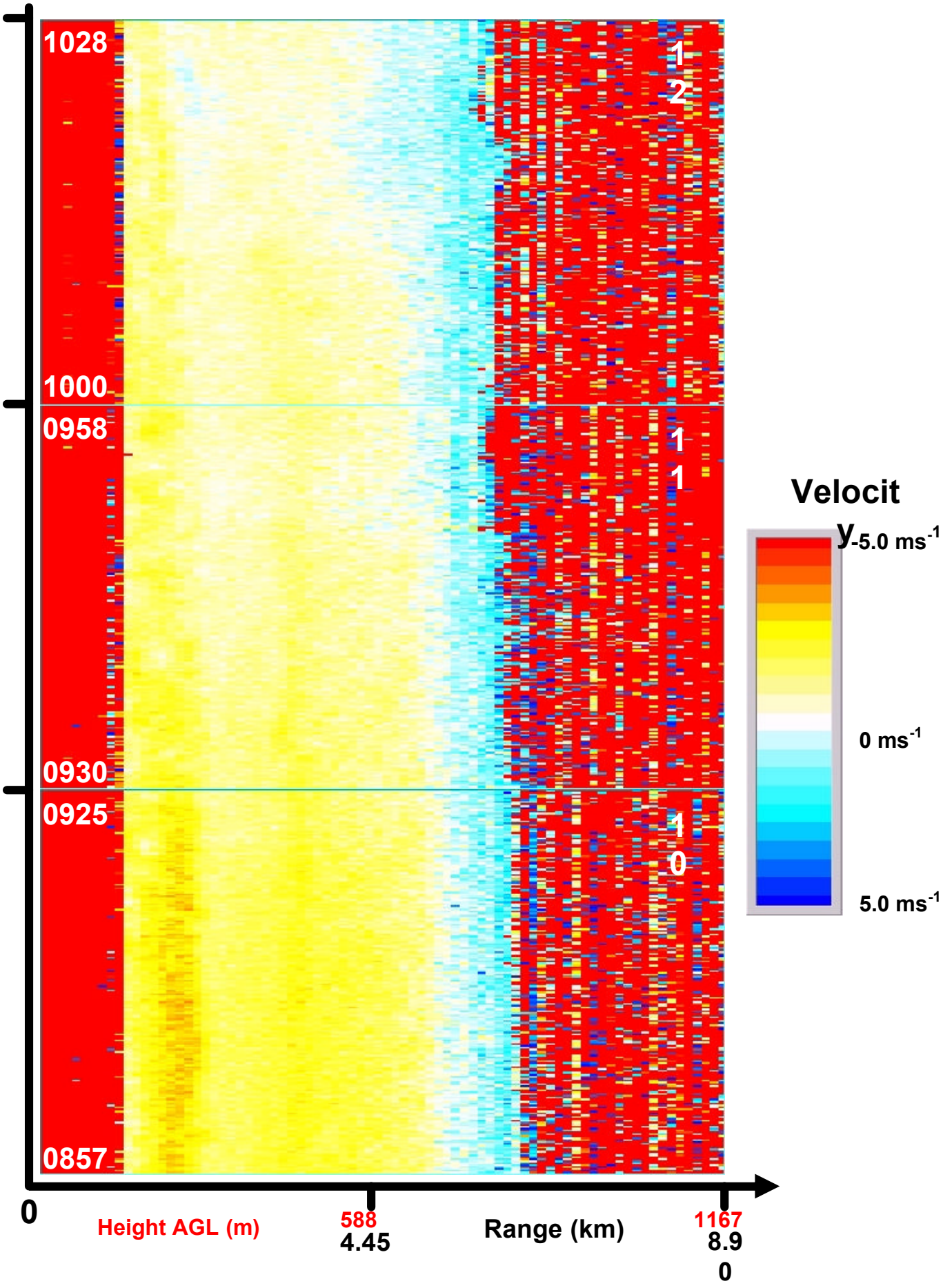

Figure (12) Range vs Velocity vs Time

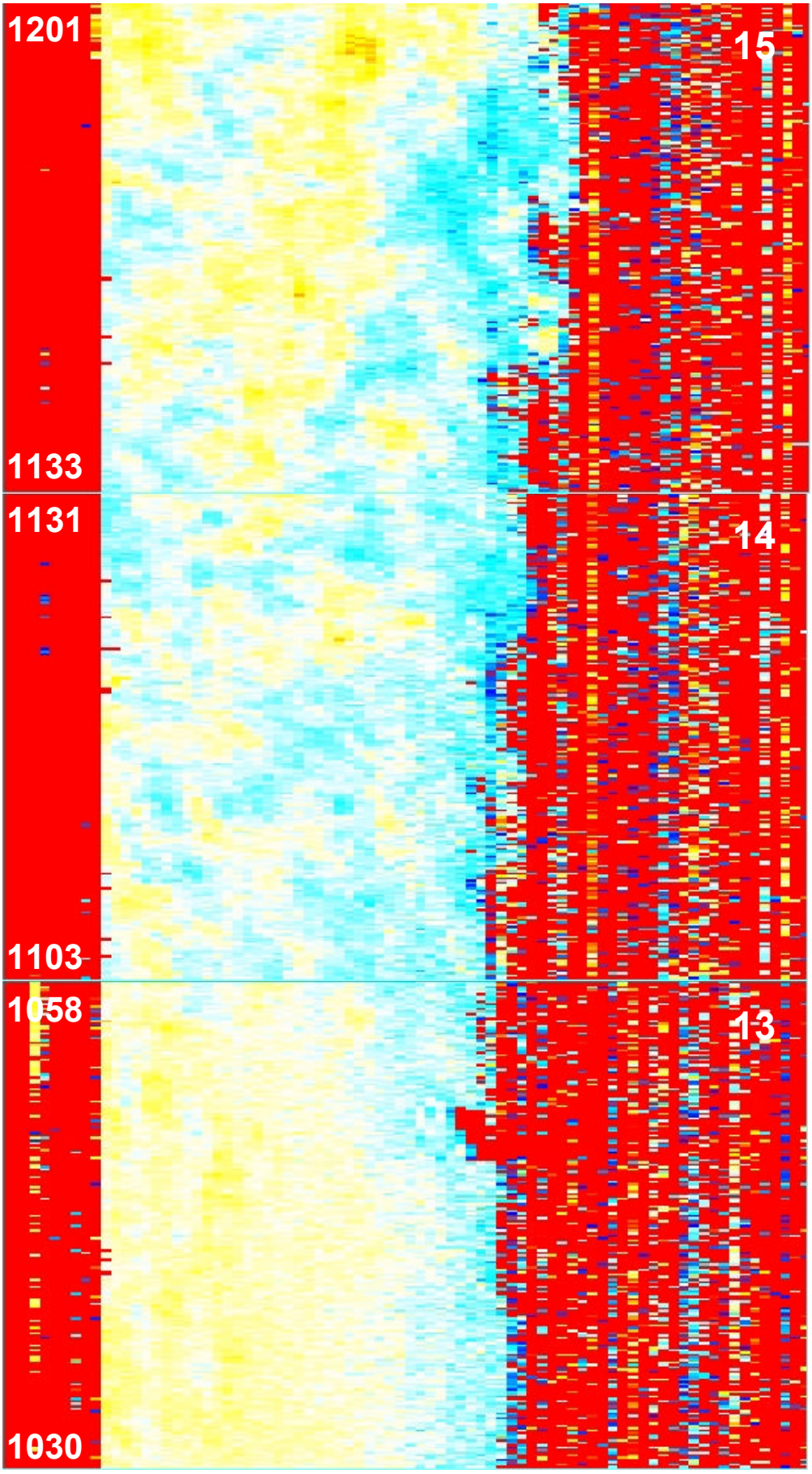
1201
1133
15
1131
1103
14
1058
1030
13

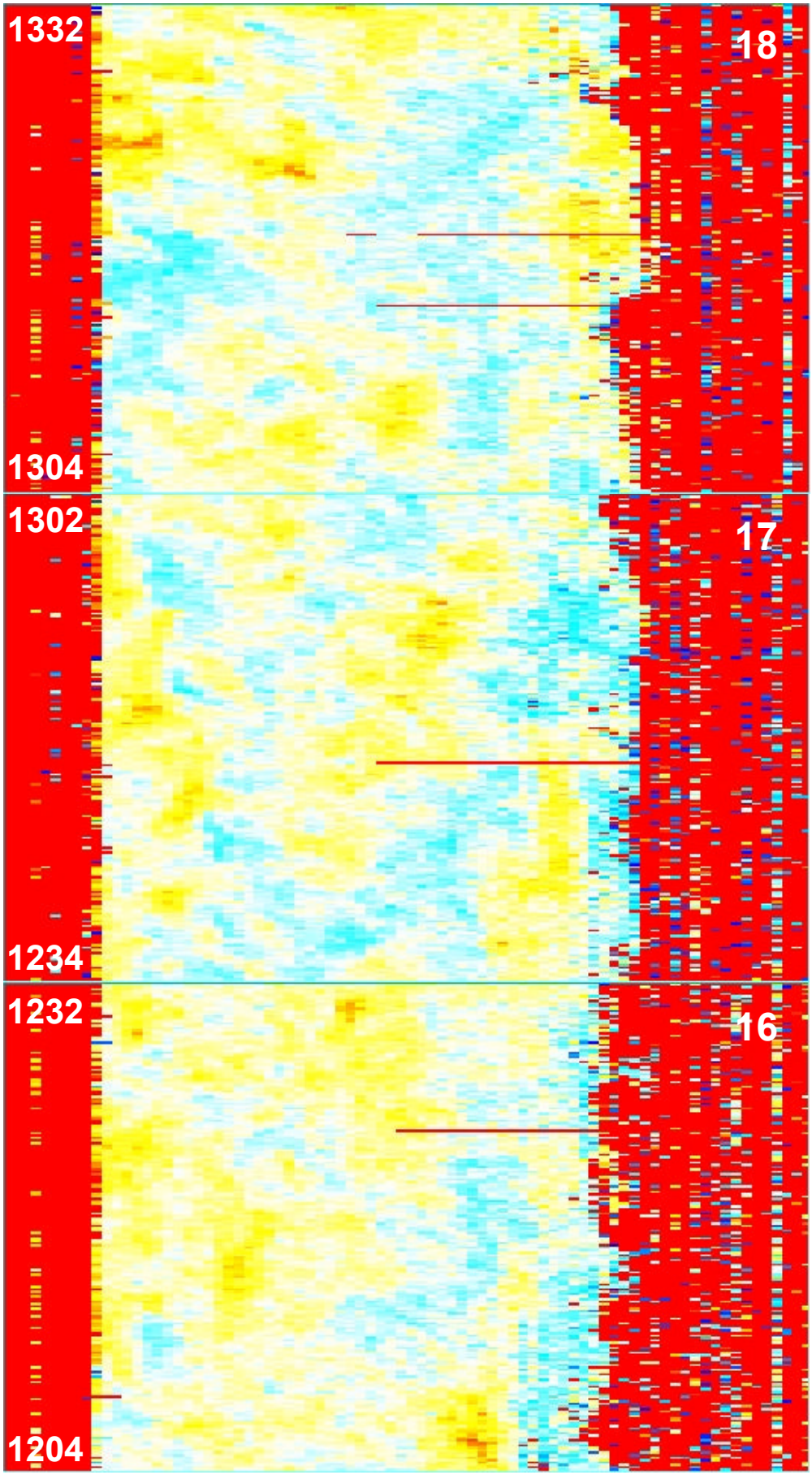

Figure (14) Range vs Velocity vs Time

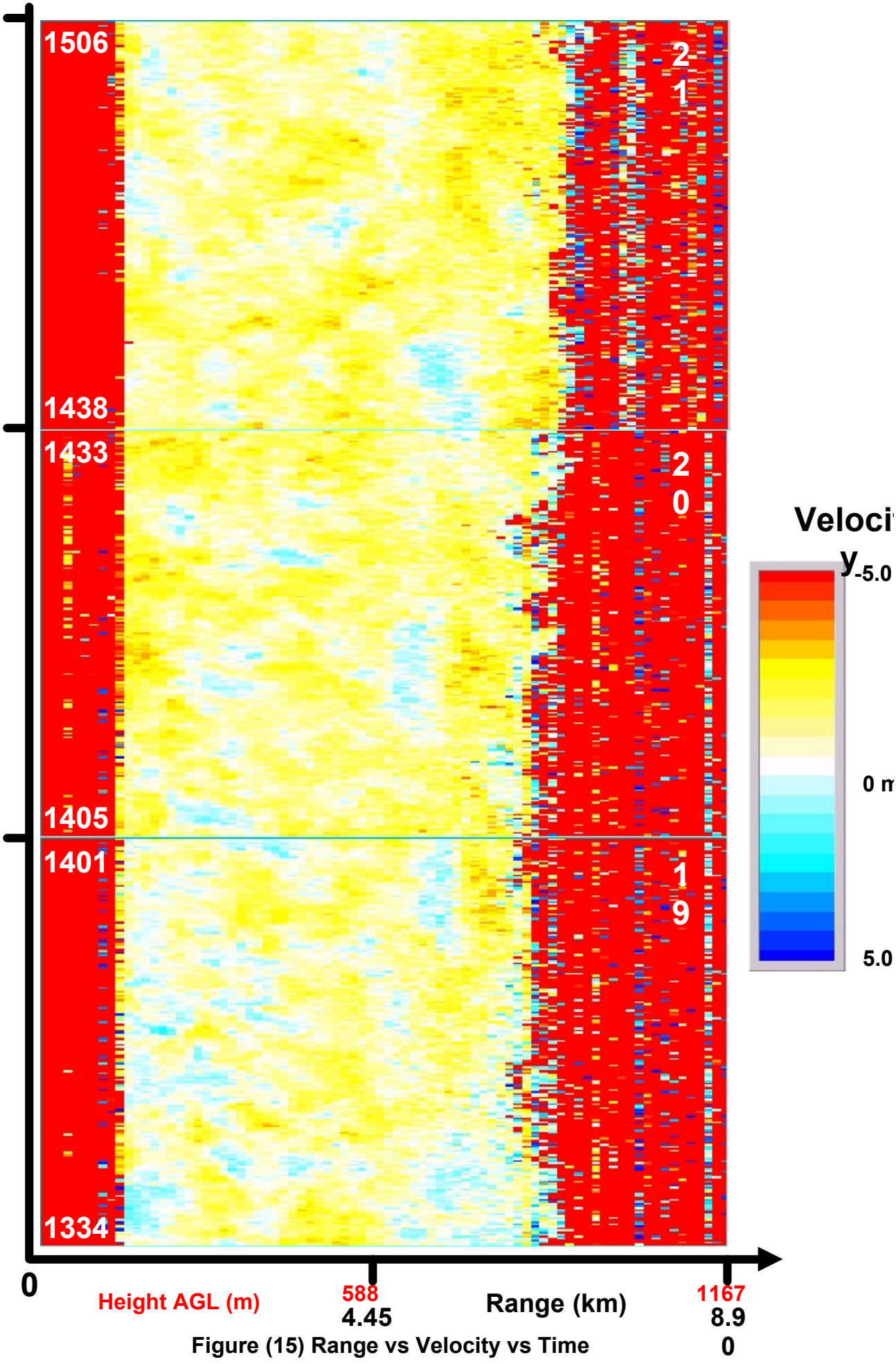

Figure (15) Range vs Velocity vs Time

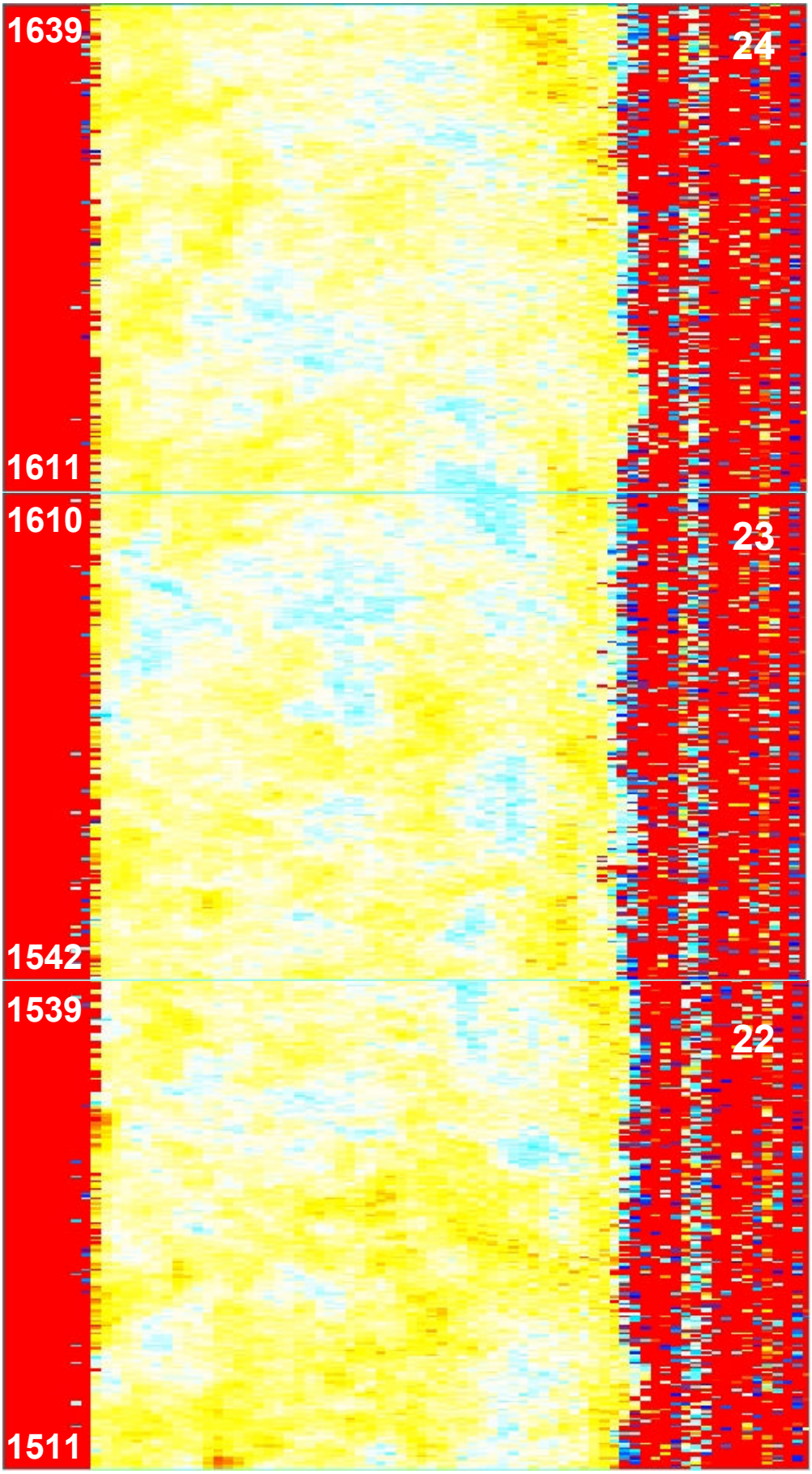

Figure (16) Range vs Velocity vs Time

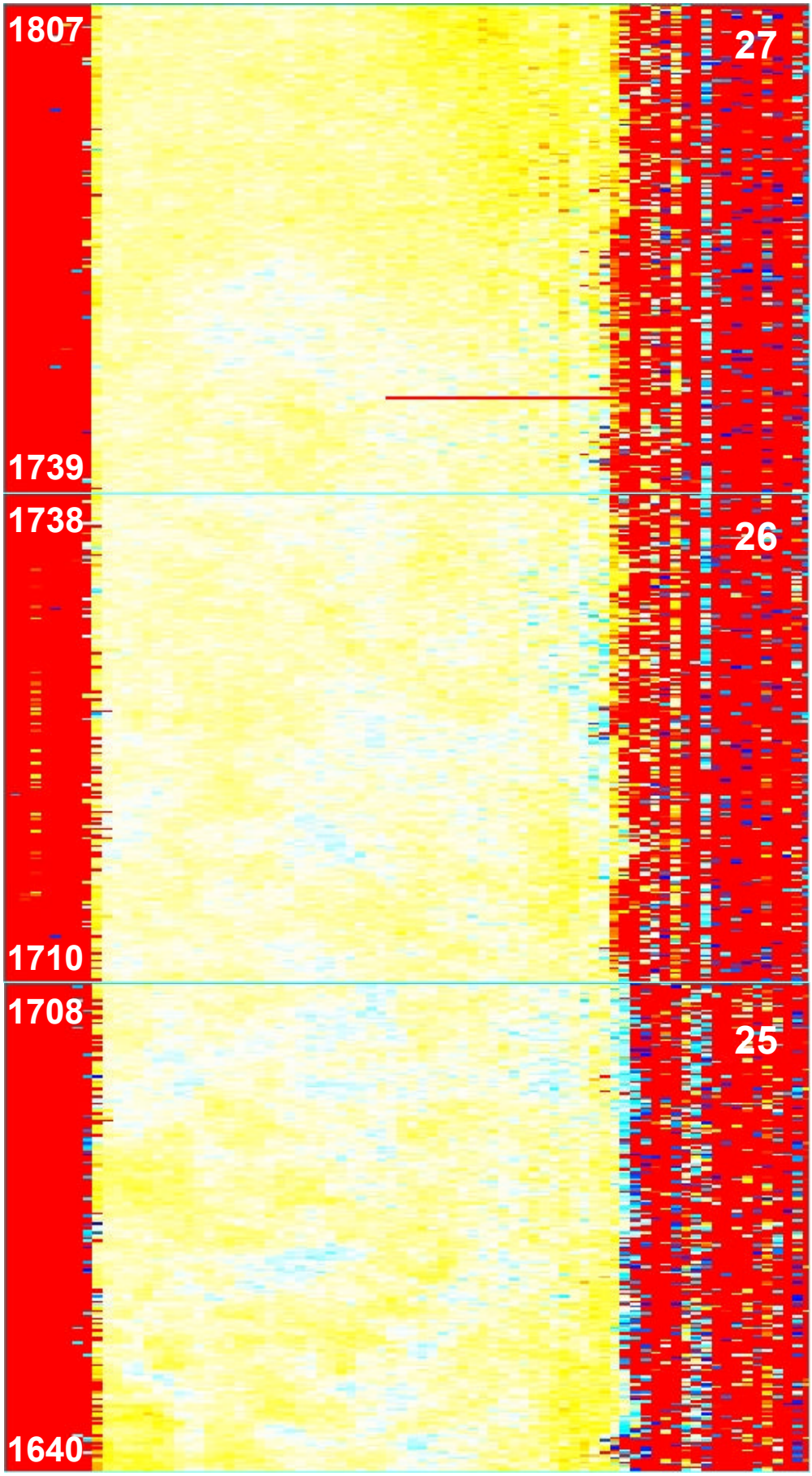

Figure (17) Range vs Velocity vs Time

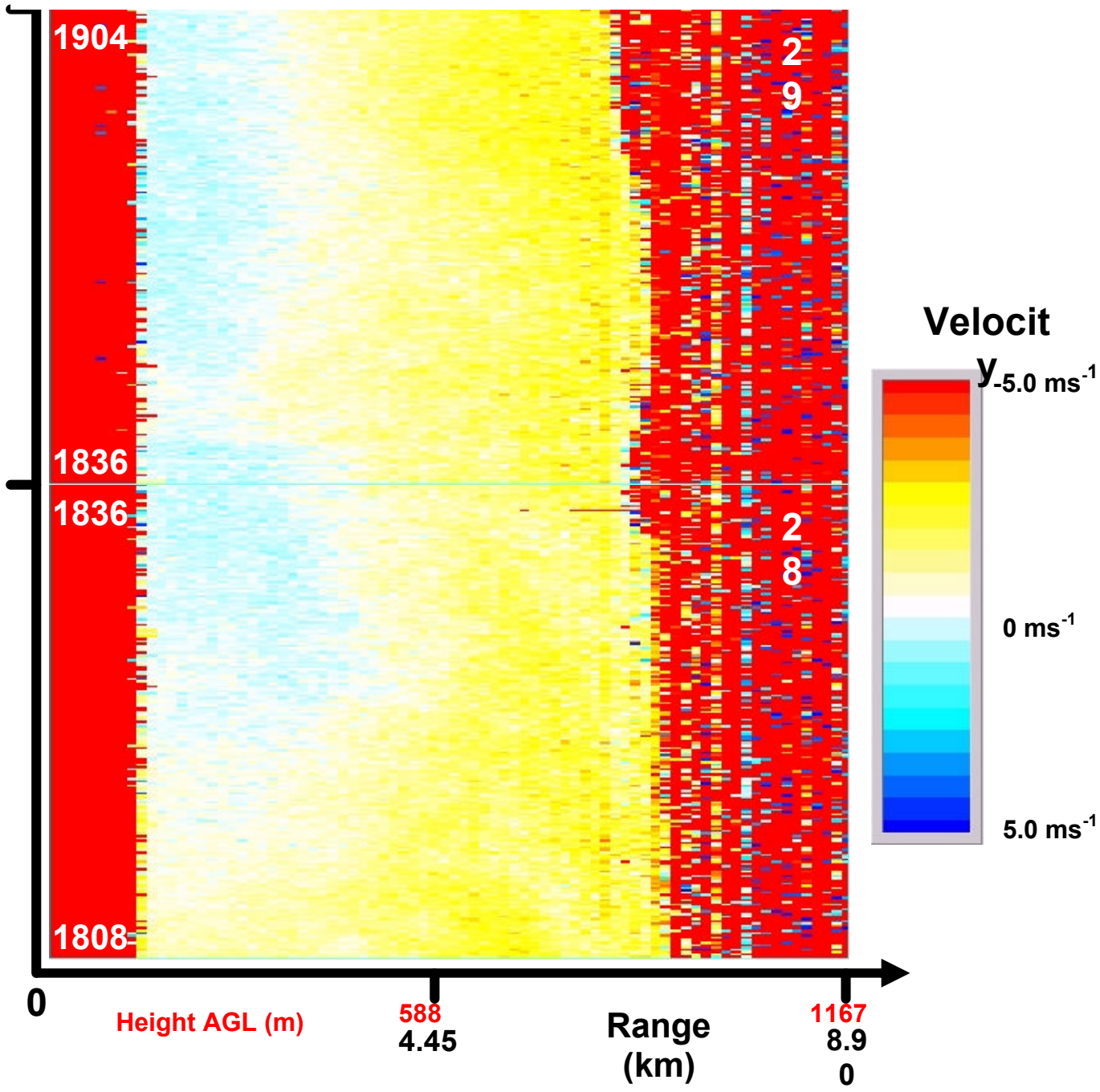

Figure (18) Range vs Velocity vs Time

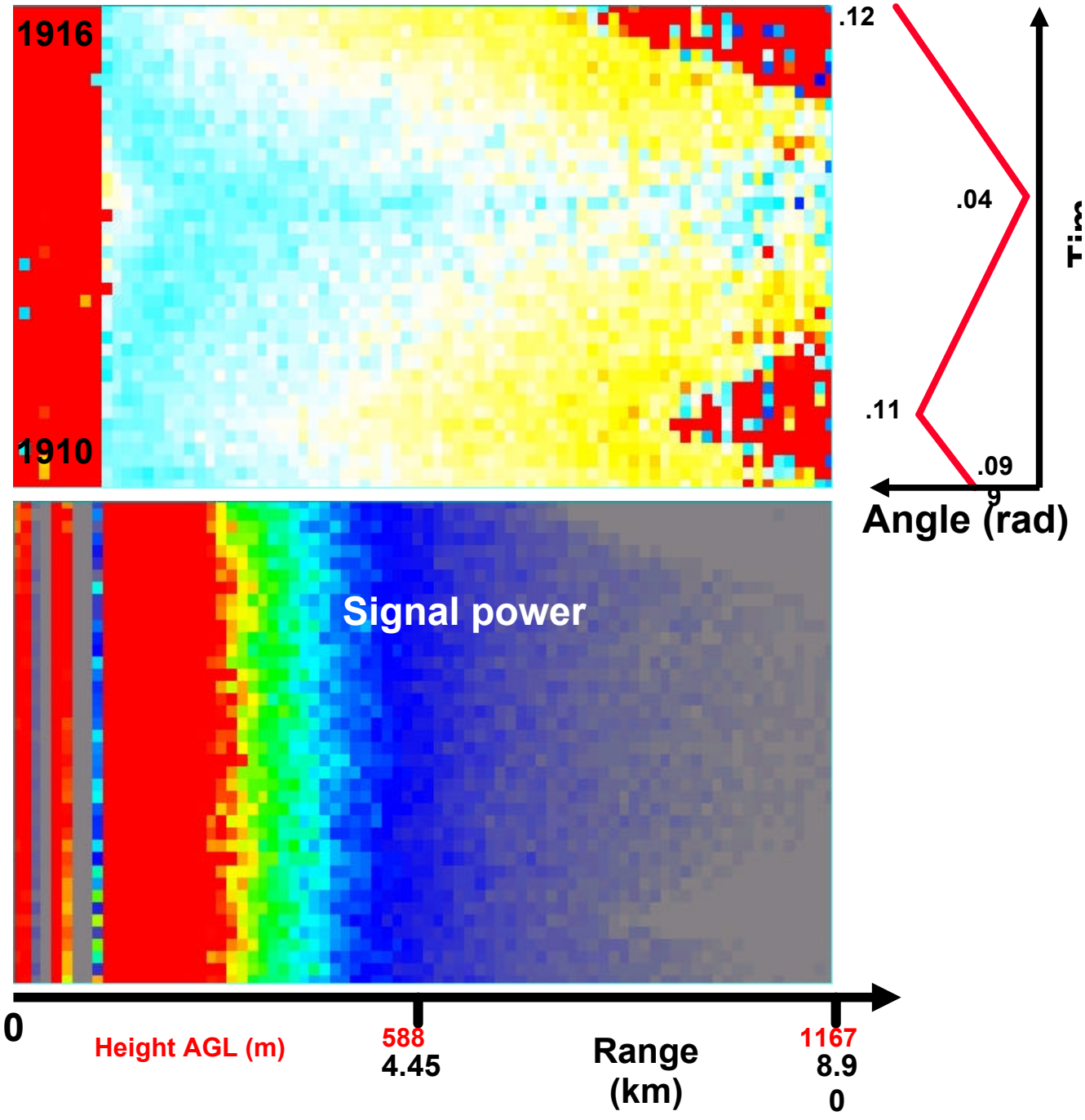

Figure (19) Range vs Velocity vs Time for a 6 minute period during which the beam was scanned.

8 Acknowledgements

This work was funded by HM Treasury under the Invest to Save Scheme. Department of Environment (DEFRA) acted on behalf of HM Treasury. QinetiQ work described herein was supported under Contract Number CU016-0000014438 and this support is acknowledged. The authors also acknowledge assistance from members of the Urban Lidar Project (Met Office, University of Essex, University of Salford) and colleagues in QinetiQ. The pulsed lidar used to make the measurements was used with the permission of Salford University. That lidar was prepared for use under contract ELM9509 between QinetiQ and Salford University.

9 Disclaimer

Distribution list

Copy No.	Name	Address
1-4	Dr Janet Dixon	DEFRA
5	Prof D V Willetts	PD315, QinetiQ Malvern
6	Dr G N Pearson	PD313, QinetiQ Malvern
Dr R I Young		PD115, QinetiQ Malvern
8-11	Dr D Middleton	Met Office, London
12	Prof C Collier	Salford University
13	Dr F Davies	Salford University
14	Dr K Bozier	Salford University
15	Prof A Holt	Essex University
16	Dr G Upton	Essex University
17	Dr S Siemen	Essex University
18	Project File	PD115, QinetiQ Malvern
19-23	Spares	PD115, QinetiQ Malvern